Received: 21 July 2021 | Revised: 2 November 2021 | Accepted: 7 November 2021

DOI: 10.1002/JPER.21-0429

JOURNAL OF Periodontology

ORIGINAL ARTICLE

LncPVT1 regulates osteogenic differentiation of human periodontal ligament cells via miR-10a-5p/brain-derived neurotrophic factor

Xiaobei Li[1] | **Yiping Huang**[1] | **Yineng Han**[1] | **Qiaolin Yang**[1] | **Yunfei Zheng**[1] | **Weiran Li**[1,2]

[1] Department of Orthodontics, Peking University School and Hospital of Stomatology, Beijing, P.R. China

[2] National Engineering Laboratory for Digital and Material Technology of Stomatology, Beijing Key Laboratory of Digital Stomatology, Beijing, P.R. China

Correspondence
Weiran Li, Department of Orthodontics, Peking University School and Hospital of Stomatology, 22 Zhongguancun Avenue South, Haidian District, Beijing 100081, P.R. China.
Email: weiranli@bjmu.edu.cn

Abstract

Background: Identifying the factors affecting osteoblast differentiation of periodontal ligament cells (PDLCs) can help enhance the regeneration of periodontal tissue. LncRNA plasmacytoma variant translocation 1 (lncPVT1) is an important regulatory factor involved in many biological processes, but its role in osteogenesis remains unclear.

Methods: Expressions of osteogenic markers were detected by quantitative reverse transcription polymerase chain reaction and Western blot analysis. Alkaline phosphatase staining was conducted for early osteoblast differentiation and alizarin red S staining was used for mineral deposition. RNA sequencing was used to identify the miRNAs regulated by lncPVT1 during osteogenesis. Cell transfection was used to overexpress or knockdown lncPVT1 and miR-10a-5p. Dual luciferase reporter assays were conducted to analyze the binding of miR-10a-5p to brain-derived neurotrophic factor (BDNF).

Results: LncPVT1 was significantly increased during osteogenic induction of PDLCs. Overexpression of lncPVT1 promoted osteogenesis, whereas lncPVT1 knockdown inhibited this process. RNA sequencing showed that miR-10a-5p expression was significantly increased after lncPVT1 knockdown. RNA immunoprecipitation assay further demonstrated the binding potential of lncPVT1 and miR-10a-5p. MiR-10a-5p inhibited the osteogenesis of PDLCs, and partially reversed the stimulatory effects of lncPVT1. Subsequently, we identified a predicted binding site for miR-10a-5p on BDNF and confirmed it using dual luciferase reporter assays. Moreover, lncPVT1 upregulated the expression of BDNF, whereas miR-10a-5p downregulated BDNF expression. BDNF promoted osteogenesis and partially rescued the si-lncPVT1-mediated inhibition of PDLCs osteogenic differentiation.

Conclusions: LncPVT1 positively regulated the osteogenic differentiation of PDLCs via miR-10a-5p and BDNF. Our results provide a promising target for enhancing the osteogenic potential of PDLCs.

KEYWORDS
brain-derived neurotrophic factor, RNA, long noncoding, microRNAs, osteogenesis, periodontal ligament, stem cells

1 | INTRODUCTION

Periodontal tissue defects are common and can lead to the loss of teeth, as well as difficulty in future treatment.[1,2] Effective periodontal tissue regeneration is an important objective of periodontal treatment.[3] Periodontal ligament cells (PDLCs), which originate from the periodontal ligament tissue, possess the self-renewal and multidirectional differentiation abilities.[4] PDLCs can form cementum/periodontal ligament-like structures, bone tissues, periodontal ligaments, peripheral nerves, and blood vessels in vivo.[5,6] Compared with other sources of stem cells, PDLCs are easier to obtain; thus, they are ideal seed cells for periodontal tissue regeneration.[7] However, the osteogenic potential of PDLCs is affected by many factors, including inflammation,[8] aging,[9] and hypoxia.[10] Therefore, identifying the factors affecting osteoblast differentiation of PDLCs will help to improve the regeneration of periodontal tissue.

Noncoding RNAs (ncRNAs) do not encode proteins, but play important roles in the regulation of gene expression at multiple levels.[11] Long noncoding RNAs (lncRNAs) are >200 nucleotides in length and regulate many important physiological and pathological activities.[12] In recent years, the roles of lncRNAs in the differentiation of stem cells have attracted attention.[13] The regulatory function of some lncRNAs in osteogenic differentiation of dental tissue-derived stem cells have also been annotated. Studies based on RNA sequencing (RNA-seq) have found that many lncRNAs are differentially expressed during osteogenic differentiation of periodontal ligament stem cells (PDLSCs)[14] and dental pulp stem cells.[15] It has been recognized that lncRNAs usually regulate osteogenesis by interacting with miRNAs. For example, lncFER1L4 promotes the osteogenic differentiation of human periodontal ligament stromal cells by binding to miR-874-3p;[16] a regulatory network composed of lncPCAT1/miR-106a-5p/E2F5 is involved in the osteogenic potential of PDLSCs;[17] and knockdown of lncMALAT1 attenuates lipopolysaccharide-induced PDLC injury by regulating miR-769-5p.[18] However, the functions and mechanisms of many other lncRNAs during osteogenesis of PDLCs remain unknown.

LncRNA plasmacytoma variant translocation 1 (lncPVT1) is an lncRNA (1.9 kb) that plays an important regulatory role in the occurrence and development of many diseases, including cancer,[19] cardiovascular disease,[20] and immune diseases.[21] However, its role in osteogenesis remains unclear. We found that lncPVT1 was continuously up-regulated during osteogenic differentiation of PDLCs in previous RNA-seq results. Therefore, in this study, the role of lncPVT1 in the osteoblast differentiation of PDLCs was investigated. The finding could reveal a new mechanism underlying the osteogenesis of PDLCs and provide new insights into periodontal tissue and bone regeneration.

2 | MATERIALS AND METHODS

2.1 | Cell culture and osteogenic induction

PDLCs were isolated and cultured from healthy premolars extracted for orthodontic reasons as described previously.[22] The premolars were collected with the informed consent of three donors. The experimental protocol was approved by the Ethics Committee of Peking University School of Stomatology (PKUSSIRB-201837096).PDLCs were cultured in growth medium (GM) containing α-modified Eagle's medium* supplemented with 10% fetal bovine serum* and 1% penicillin/streptomycin* in a humidified 5% CO_2 atmosphere at 37°C. The cells were passaged using 0.25% trypsin* and expanded until passage four for subsequent experiments. Human embryonic kidney (HEK293T) cells were commercial purchased† and cultured in Dulbecco's modified Eagle's medium* supplemented with 10% fetal bovine serum and 1% penicillin/streptomycin.

Osteogenic differentiation of PDLCs was induced using osteogenic induction medium (OM), compose of standard GM supplemented with 100 nM dexamethasone, 200 μM L-ascorbic acid, and 10 mM β-glycerophosphate‡.

* Gibco, Grand Island, NY.
* Gibco, Grand Island, NY.
* Gibco, Grand Island, NY.
* Gibco, Grand Island, NY.
† American Type Culture Collection, Manassas, VA.
* Gibco, Grand Island, NY.
‡ Sigma-Aldrich, St. Louis, MO.

2.2 | Generation of constructs

Full-length lncPVT1 cDNA was amplified and cloned into the pQLL vector[§]; the resulting pQLL-lncPVT1 construct was used for stable expression of lncPVT1.PDLCs were infected with lentivirus containing pQLL-lncPVT1 or control vector. Puromycin was used to screen stably transfected cells for further experiments.

Putative miR-10a-5p binding sites in brain-derived neurotrophic factor (BDNF) were synthesized (wild-type and mutant) and cloned downstream of the luciferase gene in luciferase vectors.[**]

2.3 | Transient cell transfection

RNA oligoribonucleotides including small-interfering RNAs (siRNAs) targeting lncPVT1 (si-lncPVT1), miR-10a-5p mimic, miR-10a-5p inhibitor, and the corresponding negative control were purchased from a commercial provider.[††] The sequences are listed in Supplementary Table S1 in the online *Journal of Periodontology*.

Transient transfection was conducted when cells reached 70% to 80% confluence using the lipofectin mediated method[‡‡], in accordance with the manufacturer's instructions. RNA oligoribonucleotides were each transfected at 100 nM; cells were harvested at specific time points for subsequent experiments.

2.4 | RNA-seq and bioinformatic analysis

PDLCs transfected with si-lncPVT1 or si-NC were cultured in six-well plates (1×10^5 cells) and osteogenic induction for 48 hours, then harvested for sequencing[§§]. Differential gene expression analysis was performed using the EBSeq package in the Bioconductor R program, as previously described.[23] Criteria for differentially expressed miRNAs were statistical significance ($P < 0.05$) and fold change >2.0. For a strict definition of differentially expressed genes, genes with normalized reads per kilo base per million mapped reads ≥1 in at least one sample were used for the analysis. The enriched Gene Ontology (GO) terms ranked by *P*-value were determined. Kyoto Encyclopedia of Genes and Genomes (KEGG) pathway analysis was performed to determine the functions of co-expressed genes in various biological pathways.

2.5 | RNA extraction and quantitative reverse-transcription polymerase chain reaction (qRT-PCR)

PDLCs were seeded into the six-well plates (1×10^5 cells). Total RNA was extracted using TRIzol reagent.[‡‡] Reverse transcription was performed using a cDNA Reverse Transcription Kit[***] with 1 μg of total RNA. miRNAs were reverse-transcribed using a specific RT primer.[†††] qRT-PCR was performed using SYBR Green Master Mix on the ABI Prism 7500 Real-Time PCR System. Glyceraldehyde 3-phosphate dehydrogenase (GAPDH) was used as the endogenous control for mRNAs and lncPVT1, whereas U6 was used as the endogenous control for miRNAs. The primers are listed in Supplementary Table S2 in the online *Journal of Periodontology*. The $2^{-\Delta\Delta CT}$ method was used to analyze the relative gene expression.

2.6 | Western blot analysis

PDLCs were seeded into the six-well plates (1×10^5 cells) and lysed with radioimmunoprecipitation assay lysis buffer containing 1.0 mM protease inhibitor cocktail to extract total protein. Equal quantities of total protein extracts were separated by 12% sodium dodecyl sulfate–polyacrylamide gel electrophoresis, then electroblotted onto polyvinylidene difluoride membranes. The membranes were blocked and incubated with primary antibodies overnight at 4°C (β-Actin[‡‡‡] [1:2500] and RUNX2[‡‡‡] [1:1000]) then incubated with the corresponding secondary antibodies[‡‡‡] (1:10,000). ImageJ software (http://rsb.info.nih.gov/ij/) was used to quantify the band intensity. The signal was normalized to β-Actin.

2.7 | Alkaline phosphatase (ALP) staining and activity

An NBT/BCIP staining kit[§§§] was used to perform ALP staining. PDLCs (5×10^4) were seeded into the 12-well plates and osteogenic induction for 7 days. Then the cells were fixed in 4% polyoxymethylene for 10 minutes and stained for ALP.

[§] HanBio. Co., Shanghai, China.
[**] Integrated Biotech Solutions Co., Shanghai, China.
[††] GenePharma Co., Shanghai, China.
[‡‡] Invitrogen, Grand Island, NY.
[§§] BGI Co., Wuhan, China.
[‡‡] Invitrogen, Grand Island, NY.
[***] Takara, Tokyo, Japan.
[†††] RiboBio, Guangzhou, China.
[‡‡‡] Abcam, Cambridge, UK.
[‡‡‡] Abcam, Cambridge, UK.
[‡‡‡] Abcam, Cambridge, UK.
[§§§] CoWin Biotech, Beijing, China.

ALP activity was analyzed using an ALP activity colorimetric assay kit.[§§§] The cultured cells were washed with phosphate-buffered saline (PBS), lysed with 1% Triton X-100, and scraped into distilled water. The absorbance was detected at 405 nm using p-nitrophenyl phosphate as the substrate. Total protein concentrations were determined by the bicinchoninic acid method[****]. ALP activity was calculated from the absorbance levels relative to the protein concentration.

2.8 | Alizarin red S (ARS) staining and quantification

Mineralized nodule formation was determined by ARS staining. PDLCs (5×10^4) were seeded into the 12-well plates. After osteogenic induction for 14 days, cells were fixed in 4% polyoxymethylene for 10 minutes and washed with distilled water, then stained with 0.1% ARS (pH = 4.2)[‡] for 20 minutes. For quantitative assessment of the mineralized nodules, the stain was dissolved with 1 mL 10% cetylpyridinium chloride[‡] for 1 hour, then quantified by spectrophotometric absorbance at 570 nm. ARS intensity was normalized to the total protein concentration.

2.9 | RNA immunoprecipitation (RIP) assay

An RNA-binding protein immunoprecipitation kit[††††] was used to determine the relationship between lncPVT1 and miR-10a-5p, according to the manufacturer's instructions. Antibodies used for the RIP assay included anti-Ago2[‡‡‡] and control IgG[††††]. The coprecipitated RNAs were used for cDNA synthesis and evaluated via qRT-PCR.

2.10 | Dual luciferase reporter assay

Luciferase assays were performed as described previously.[24] Briefly, 40 ng of BDNF luciferase reporter plasmid was transfected into HEK293T cells with 10 pmol miR-NC or miR-10a-5p mimic. After cells had been incubated for 24 hours, they were washed with PBS and protein extracts were collected with 1x passive lysis buffer. Then Renilla and Firefly luciferase activities were measured using the dual luciferase reporter assay system[‡‡‡‡]. The light intensity from Renilla luciferase was normalized to the light intensity from Firefly luciferase, then expressed as fold-induction relative to basal activity.

2.11 | Enzyme-linked immunosorbent assay (ELISA)

The protein level of BDNF in the culture supernatants was determined using an ELISA kit[§§§§]. Briefly, the cell culture supernatants were collected and added to ELISA plates that had been coated with a primary antibody against human BDNF. After the plates had been incubated for 2 hours, they were washed four times. Then, plates were incubated with secondary antibodies for 1 hour. Horseradish peroxidase-conjugated streptavidin was added, followed by the addition of 3,3′,5,5′-tetramethylbenzidine substrate solution. Finally, the stop solution was added to terminate the reaction. The optical density was detected at 450 nm.

2.12 | Statistical analysis

SPSS version 16.0 software[*****] was used for statistical analysis. All data are expressed as the means ± standard deviations of at least three independent experiments. Student's *t*-test was used to analyze differences between groups. One-way analysis of variance was used to analyze differences among multiple groups. A two-tailed value of $P < 0.05$ was considered statistically significant.

3 | RESULTS

3.1 | LncPVT1 was upregulated during osteoblast differentiation of PDLCs

After osteogenic induction for 0, 3, 7, and 14 days, mRNA expression levels of ALP, RUNX2, and OCN were significantly increased during osteogenic induction, indicating the successful induction of PDLCs to undergo osteoblast differentiation (Figure 1A). Dynamic expression profiles of lncPVT1 in PDLCs were then detected during osteogenic induction. LncPVT1 was significantly upregulated during osteogenic induction (Figure 1B). There were significant positive correlations between lncPVT1 expression and the expression levels of ALP, RUNX2, and OCN (Figure 1C),

§§§ CoWin Biotech, Beijing, China.
**** Thermo Fisher Scientific, Rockford, IL.
‡ Sigma-Aldrich, St. Louis, MO.
‡ Sigma-Aldrich, St. Louis, MO.
†††† Millipore, Billerica, MA.
‡‡‡ Abcam, Cambridge, UK.
†††† Millipore, Billerica, MA.
‡‡‡‡ Promega, Beijing, China.
§§§§ Proteintech, Beijing, China.
***** SPSS, Chicago, IL.

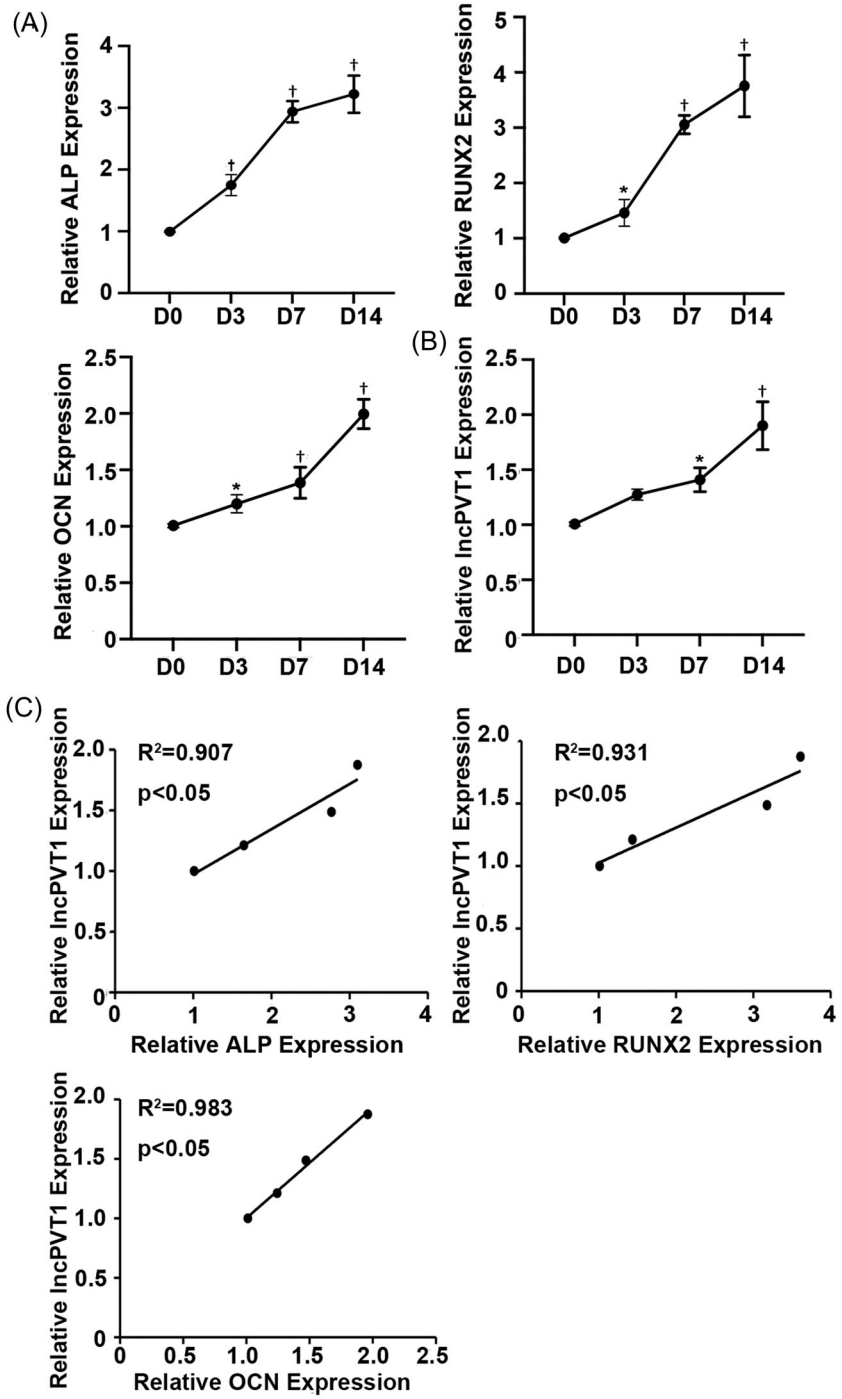

FIGURE 1 Expression pattern of lncPVT1 during osteogenic differentiation of PDLCs. (**A**) Relative mRNA expression of the osteogenic markers ALP, RUNX2 and OCN at 0, 3, 7, and 14 days of osteogenic induction as determined by qRT-PCR analysis. GAPDH was used as an internal control, relative to day 0 groups. (**B**) Relative expression of lncPVT1 during osteogenic differentiation of PDLCs at the indicated time points. (**C**) Correlation analyses were performed between lncPVT1 levels and ALP, RUNX2, and OCN mRNA levels during osteogenic differentiation. Results are presented as mean ± SD (*$P < 0.05$, †$P < 0.01$). GAPDH, glyceraldehyde 3-phosphate dehydrogenase; ALP, alkaline phosphatase; RUNX2, Runt-related transcription factor 2; OCN, osteocalcin

suggesting that lncPVT1 is involved in the osteoblast differentiation of PDLCs.

3.2 | LncPVT1 promoted osteogenic differentiation of PDLCs

To determine the function of lncPVT1 in the osteoblast differentiation of PDLCs, lncPVT1 was overexpressed using the pQLL-lncPVT1 vector and knocked down using si-lncPVT1. qRT-PCR analysis confirmed that the expression of lncPVT1 was knocked down by ≈50% in knockdown group and increased by ≈ 10-fold in overexpression group (Figure 2A, 2B). After osteogenic induction for 48 hours, qRT-PCR analysis indicated that the mRNA expression levels of ALP, RUNX2, and OCN were significantly decreased in the lncPVT1 knockdown group (Figure 2A) and significantly increased in the overexpression group (Figure 2B). Western blotting revealed that the protein level of RUNX2 was decreased in the knockdown group and increased in the overexpression group (Figure 2C, 2D). Following osteogenic induction for 7 days, ALP staining and activity were decreased with lncPVT1 knockdown and increased

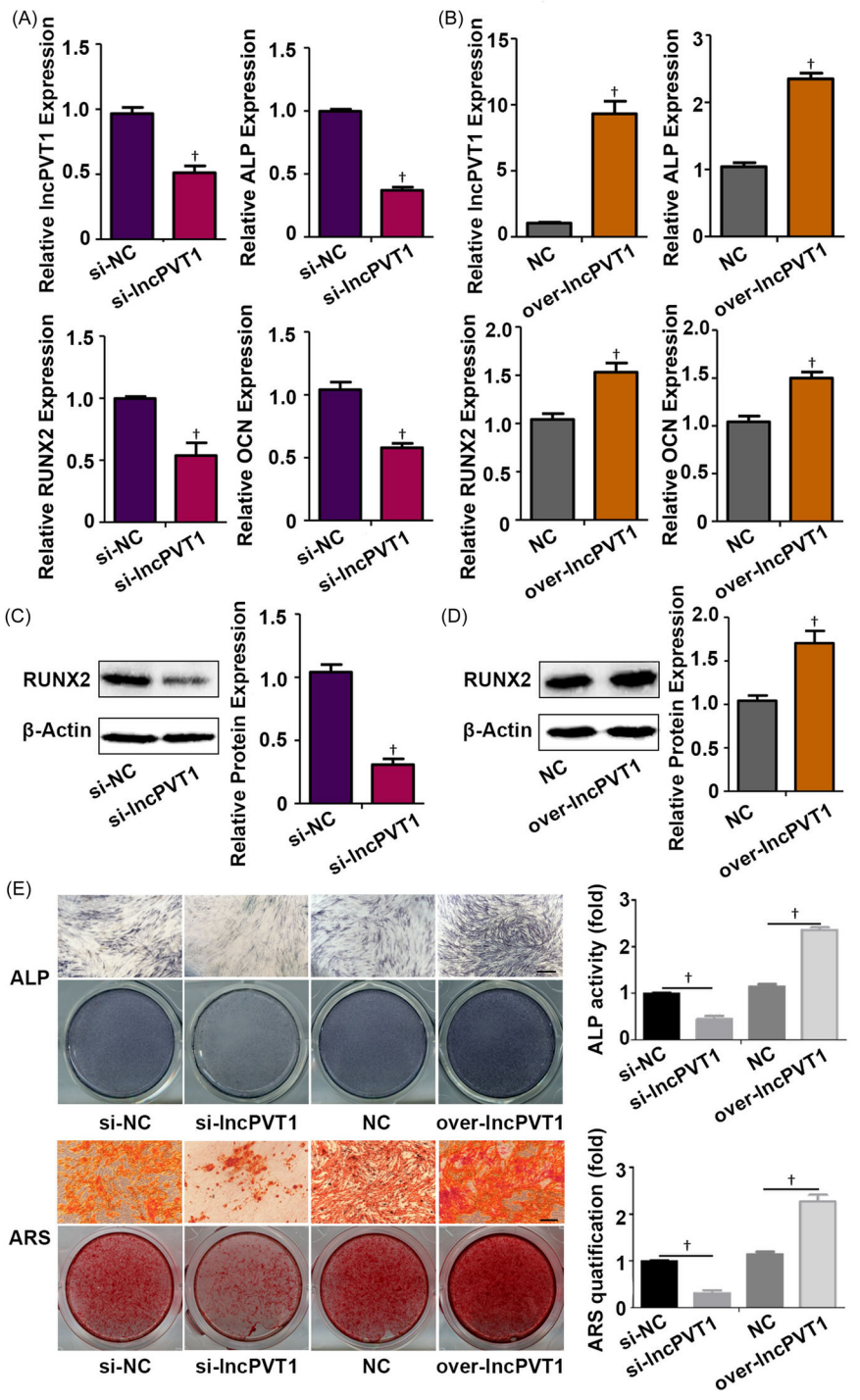

FIGURE 2 LncPVT1 promoted the osteogenic differentiation of PDLCs. (**A**) Efficiency of transient transduction of si-lncPVT1 and relative mRNA expression of ALP, RUNX2 and OCN measured by qRT-PCR at day 3 of osteogenic induction. GAPDH was used for normalization, relative to si-NC groups. (**B**) Overexpression efficiency of pQLL-lncPVT1 and relative mRNA expression of ALP, RUNX2, and OCN. GAPDH was used for normalization, relative to NC groups. (**C**, **D**) Western blot analysis of protein expression of RUNX2 and the internal control β-Actin at day 3 of osteogenic induction. Histograms show the quantification of band intensities. β-Actin was used for normalization, relative to si-NC or NC groups. (**E**) Left: Images of ALP staining on day 7 of osteogenic differentiation and ARS staining on day 14 of osteogenic differentiation in the si-lncPVT1 groups, over-lncPVT1 groups and corresponding control groups. Right: Histograms of ALP activity and quantification of ARS staining by spectrophotometry. Normalized to the si-NC or NC groups. Scale bar, 100 μm ($^{*}P < 0.05$; $^{\dagger}P < 0.01$). si-NC, negative control for siRNA; si-lncPVT1, siRNA targeting lncPVT1; NC, negative control for pQLL-lncPVT1; over-lncPVT1, cells were transfected with a vector expressing lncPVT1 (pQLL-lncPVT1) to overexpression of lncPVT1; ARS, Alizarin Red S

with lncPVT1 overexpression. After osteogenic induction for 14 days, the intensity of ARS staining showed a similar trend, indicating that the matrix mineralization of PDLCs was regulated by lncPVT1 (Figure 2E).

3.3 | MiR-10a-5p was a target miRNA of lncPVT1

To identify target miRNAs regulated by lncPVT1 during osteogenesis of PDLCs, we detected the expression patterns of miRNAs after lncPVT1 knockdown by RNA-seq. Figure 3A presents a heat map showing the miRNA expression profiles. Compared to the control group, 29 miRNAs were upregulated and 15 miRNAs were downregulated after lncPVT1 knockdown. The expression levels of five differentially expressed miRNAs were validated by qRT-PCR; the results were consistent between the qRT-PCR and RNA-seq analyses (Figure 3B). KEGG pathway analysis showed that the co-expressed genes of the differentially expressed miRNAs were associated with metabolic

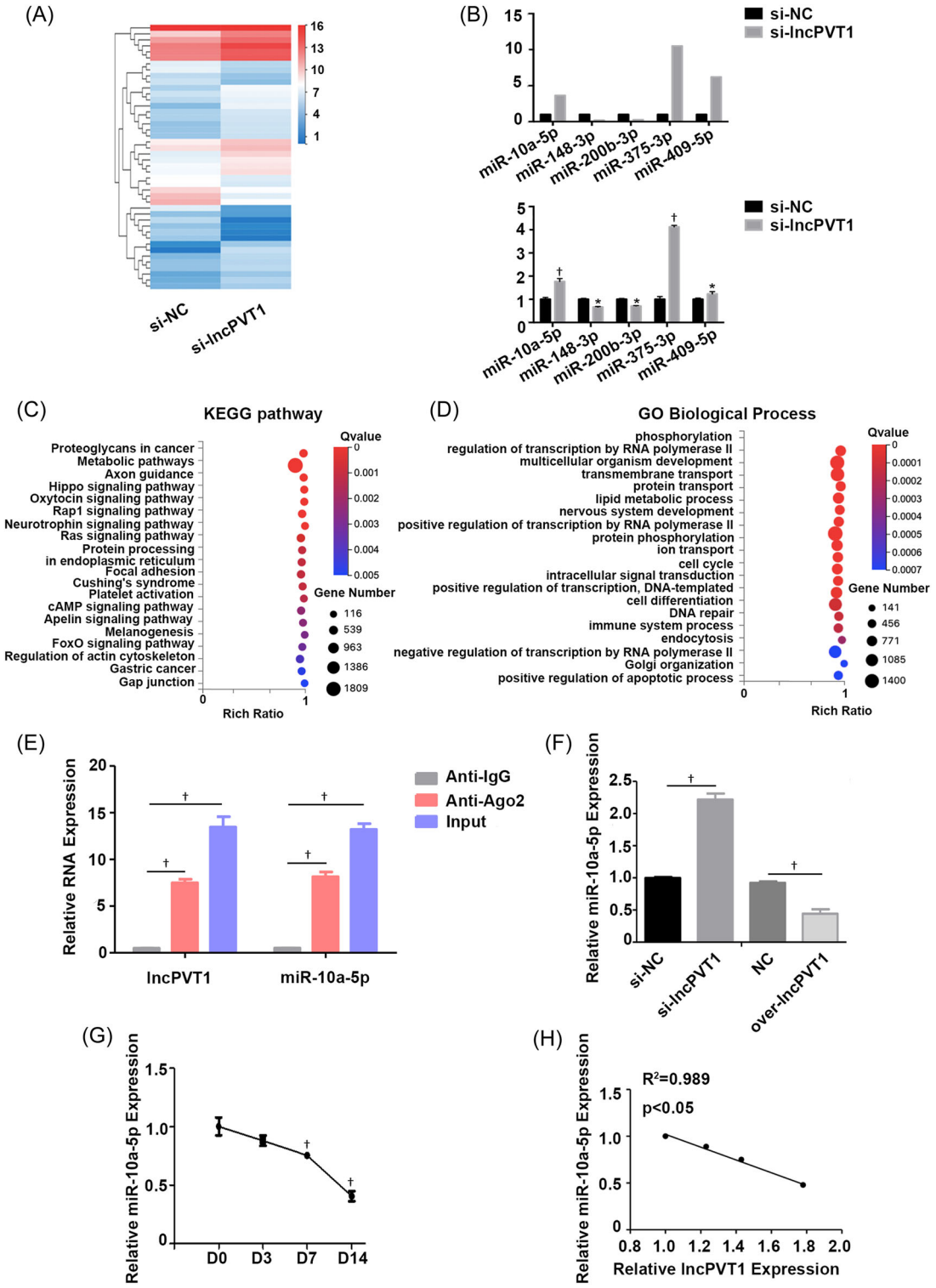

FIGURE 3 Mir-10a-5p was a target miRNA of lncPVT1. (**A**) Overall expression profiles of miRNAs in si-NC and si-lncPVT1 groups were presented by a heat map. (**B**) The relative expression of miR-10a-5p, miR-148-3p, miR-200b-3p, miR-375-3p, and miR-409-5p was consistent between qRT-PCR and RNA sequencing. (**C**) KEGG pathway analysis showed the related mRNAs were enriched in the metabolic pathways. (**D**) Enriched GO terms of the host genes of differentially expressed miRNAs. (**E**) RIP assay results showed the enrichment of lncPVT1 and miR-10a-5p using qRT-PCR in Ago2 protein pulldown samples. (**F**) The relative expression of miR-10a-5p when lncPVT1 was overexpressed or knocked down. U6 was used as an internal control, relative to the si-NC or NC groups. (**G**) Dynamic expression profile of miR-10a-5p in PDLCs at 0, 3, 7, and 14 days of osteogenic induction. Normalized to the day 0 groups. (**H**) Correlation analyses between miR-10a-5p levels and lncPVT1 levels during osteogenic induction (*$P < 0.05$; †$P < 0.01$). KEGG pathway, Kyoto Encyclopedia of Genes and Genomes pathway analysis; GO, Gene Ontology

pathways (Figure 3C). GO analysis showed that the host genes of the differentially expressed miRNAs were associated with cell differentiation and protein transport or phosphorylation (Figure 3D). The RIP assay showed that the Ago2 antibody was able to pull down both endogenous lncPVT1 and miR-10a-5p (Figure 3E), validating the binding potential of lncPVT1 and miR-10a-5p. The qRT-PCR results of the RIP assay were also confirmed by electrophoresis (see Supplementary Figure S1 in online *Journal of Periodontology*). Furthermore, qRT-PCR analysis showed that miR-10a-5p expression was increased after knockdown of lncPVT1 and decreased after overexpression of lncPVT1 (Figure 3F). Besides, miR-10a-5p expression was also gradually decreased during osteogenic induction (Figure 3G), and there was a negative correlation between miR-10a-5p and lncPVT1 expression during osteogenesis (Figure 3H).

3.4 | MiR-10a-5p inhibited osteoblast differentiation of PDLCs

To determine whether miR-10a-5p was involved in the osteogenesis process, transient transfection was conducted to overexpress or knockdown miR-10a-5p. qRT-PCR showed that miR-10a-5p expression was increased by ≈ 70,000-fold in the overexpression group and knocked down by >99% in the knockdown group (Figure 4A). Western blotting confirmed that overexpression of miR-10a-5p decreased the protein level of RUNX2, whereas knockdown of miR-10a-5p increased RUNX2expression (Figure 4B). mRNA expression levels of the osteogenic markers ALP, RUNX2, and OCN were decreased in the miR-10a-5p overexpression group and increased in the knockdown group (Figure 4C). ALP staining and activity were significantly decreased when miR-10a-5p was overexpressed and increased when miR-10a-5p was knocked down. Matrix mineralization of PDLCs also showed a similar trend as determined by ARS staining (Figure 4D). These results suggest that miR-10a-5p inhibited the osteogenesis of PDLCs.

3.5 | MiR-10a-5p partially blocked the pro-osteogenic function of lncPVT1

To further confirm whether lncPVT1 mediated osteogenic differentiation of PDLCs by regulating miR-10a-5p, we transfected miR-10a-5p mimic or inhibitor into PDLCs stably overexpressing lncPVT1 and undergo osteogenic induction. The miR-10a-5p mimic partially blocked the upregulation of ALP, RUNX2, and OCN expression by lncPVT1, whereas the miR-10a-5p inhibitor further promoted the upregulation of these genes (Figure 5A). Moreover, the miR-10a-5p mimic partially reversed the ability of lncPVT1 to promote the osteoblast differentiation of PDLCs, whereas the miR-10a-5p inhibitor further promoted this phenomenon, as revealed by ALP and ARS staining (Figure 5B).

3.6 | BDNF was regulated by lncPVT1/miR-10a-5p

To uncover the downstream molecular mechanism contributing to lnc-PVT1/miR-10a-5p-mediated regulation of osteogenesis, we used target-prediction algorithms (miRanda and TargetScan software) to identify potential targets of miR-10a-5p. Notably, we found that the 3′-untranslated region (UTR) region of the osteogenic gene BDNF contained miR-10a-5p binding sites (Figure 6A). Next, we constructed two types of luciferase reporters for BDNF: the wild-type reporter contained the wild-type 3′-UTR of BDNF, whereas the mutant reporter contained a 3′-UTR with a mutated miR-10a-5p binding site. The miR-10a-5p mimic remarkably decreased luciferase activity in the wild-type group; this reduced activity was not observed when the 3′-UTR was mutated (Figure 6B). In addition, qRT-PCR analysis showed that the overexpression of lncPVT1 or knockdown of miR-10a-5p increased mRNA expression levels of BDNF, whereas knockdown of lncPVT1 or overexpression of miR-10a-5p decreased mRNA expression levels of BDNF. Moreover, there were no significant changes in BDNF expression when miR-10a-5p and lncPVT1 were overexpressed or knocked down simultaneously (Figure 6C). ELISA analysis revealed that protein levels of BDNF showed a similar trend (Figure 6D), confirming that BDNF is regulated by lncPVT1/miR-10a-5p.

3.7 | BDNF promoted o steoblast differentiation of PDLCs and partially rescued the si-lncPVT1-mediated inhibition of osteogenesis

The expression pattern of BDNF during osteogenic differentiation of PDLCs was detected by qRT-PCR and ELISA. The results showed that BDNF was gradually upregulated during osteogenic induction (see Supplementary Figure S2 in online *Journal of Periodontology*). To further verify the effect of BDNF on osteogenic differentiation of PDLCs, various concentrations of BDNF were added to the culture medium to induce osteogenesis. qRT-PCR results showed that BDNF could significantly increase the expression levels of ALP, RUNX2, and OCN (Figure 6E). Western blotting showed that protein levels of RUNX2 were increased

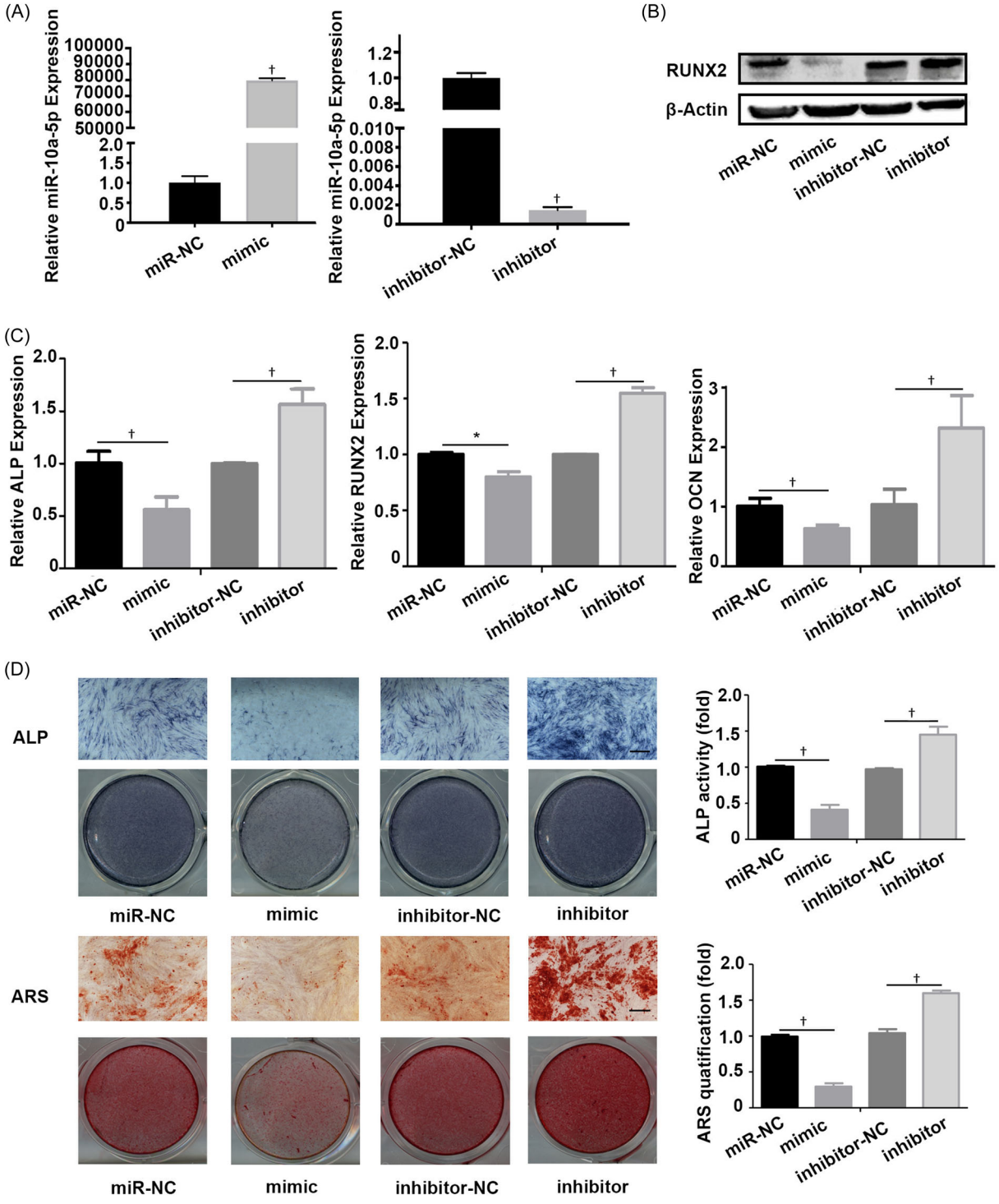

FIGURE 4 MiR-10a-5p inhibited osteogenic differentiation of PDLCs. (**A**) qRT-PCR confirmed the efficiency of transient transduction of miR-10a-5p mimic and inhibitor. U6 was used for normalization, relative to miR-NC or inhibitor-NC groups. (**B**) Western blot analysis of protein expression of RUNX2 and the internal control β-Actin at day 3 of osteogenic induction. (**C**) Relative mRNA expression of ALP, RUNX2 and OCN measured by qRT-PCR at day 3 of osteogenic induction. GAPDH was used for normalization. (**D**) Left: Images of ALP staining at day 7 of osteogenic differentiation and ARS staining at day 14 of osteogenic differentiation in the miR-10a-5p mimic groups, miR-10a-5p inhibitor groups and corresponding control groups. Right: Histograms show ALP activity and quantification of ARS staining by spectrophotometry. Normalized to the miR-NC or inhibitor-NC groups. Scale bar, 100 μm (*$P < 0.05$; $^{\dagger}P < 0.01$)

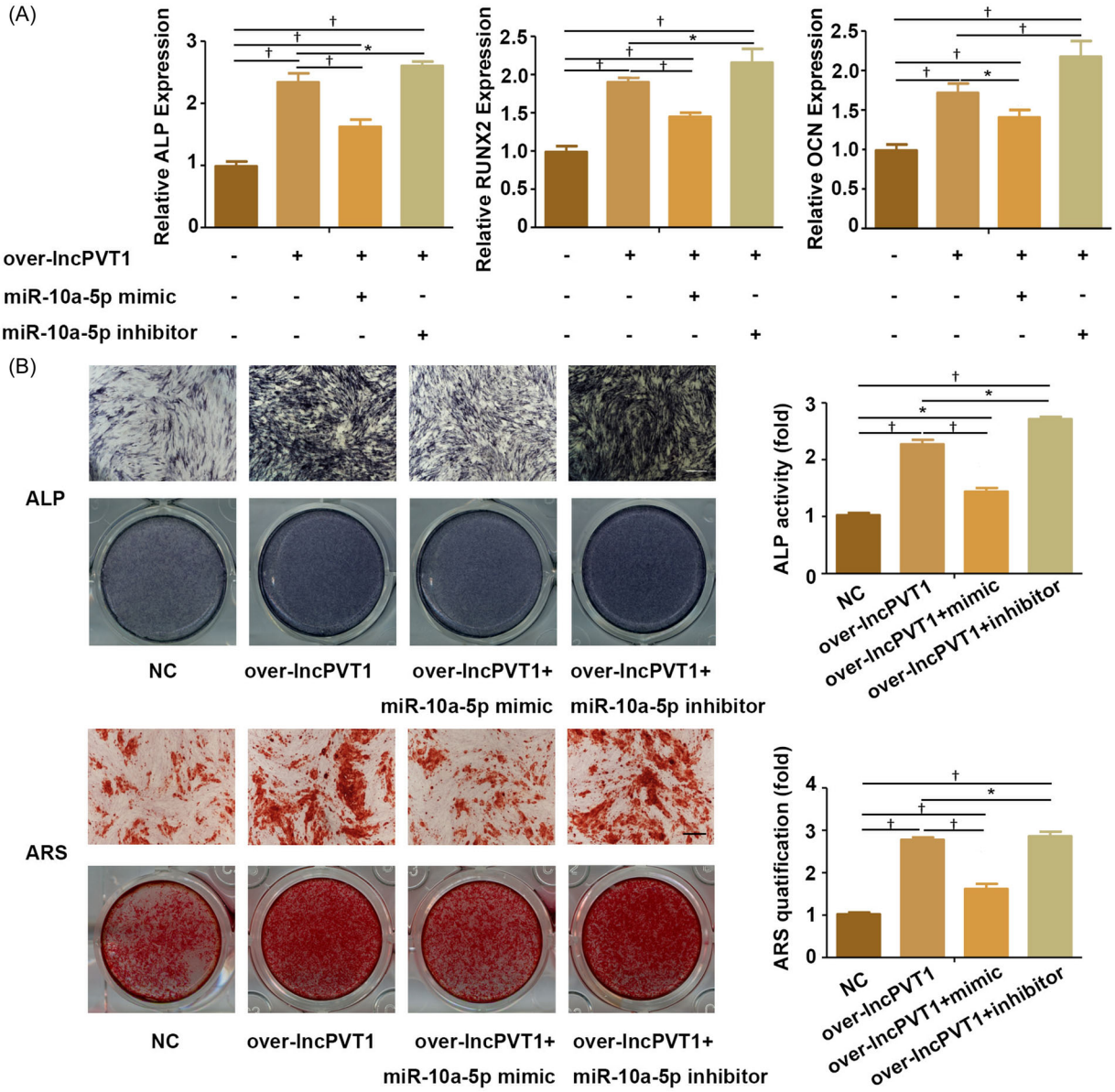

FIGURE 5 MiR-10a-5p partially blocked the pro-osteogenic function of lncPVT1. (**A**) qRT-PCR showed the relative expression of osteogenic markers ALP, RUNX2, and OCN in PDLCs co-transfected with pQLL-lncPVT1 with or without miR-10a-5p. (**B**) Left: Images of ALP staining on day 7 of osteogenic differentiation and ARS staining on day 14 of osteogenic differentiation in the NC groups, lncPVT1 overexpression groups, co-transfected with pQLL-lncPVT1 and miR-10a-5p mimic group and co-transfected with pQLL-lncPVT1 and miR-10a-5p inhibitor groups. Right: Histograms show ALP activity and quantification of ARS staining by spectrophotometry. Scale bar, 100 μm (*$P < 0.05$; $^{\dagger}P < 0.01$)

in BDNF-treated groups, and the inhibitory effect of si-lncPVT1 on RUNX2 expression in PDLCs was partially rescued by the addition of BDNF (Figure 6F). ALP and ARS staining also showed that BDNF could promote the osteogenic differentiation of PDLCs and 50 ng/mL BDNF had a stronger effect. In addition, BDNF could partially reverse the inhibitory effect of si-lncPVT1 on osteogenesis (Figure 6G).

4 | DISCUSSION

In this study, we demonstrated that lncPVT1 promotes osteoblast differentiation of PDLCs. LncPVT1 was continuously upregulated during osteoblast differentiation of PDLCs; its expression level was positively correlated with the osteogenic markers, suggesting that lncPVT1 was

JOURNAL OF Periodontology

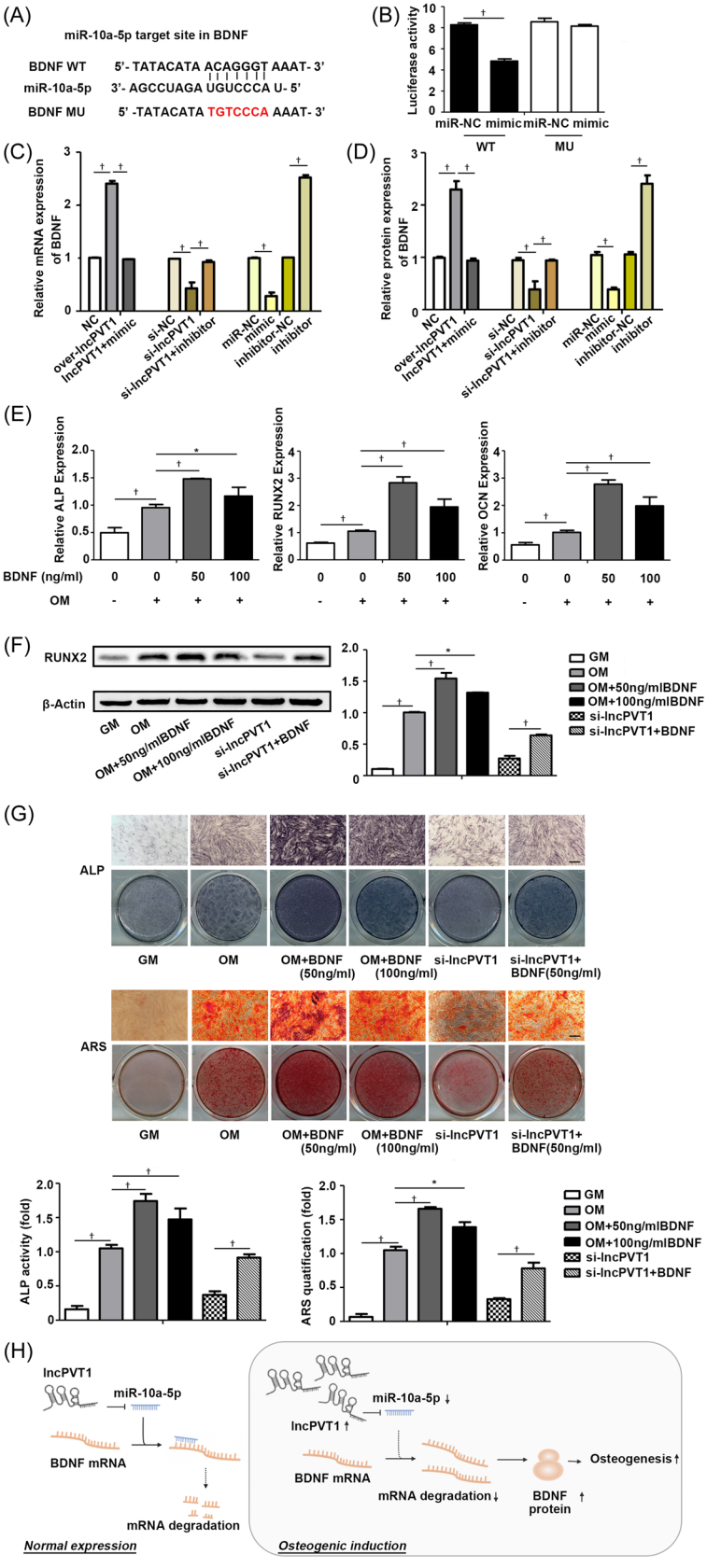

FIGURE 6 BDNF was regulated by lncPVT1/miR-10a-5p and partially rescued the si-lncPVT1-mediated inhibitionof osteogenesis. (**A**) Schematic diagram of the miR-10a-5p putative binding site in WT and MU BDNF 3′-UTR. (**B**) Relative luciferase activities of luciferase reporters containing WT or MU BDNF 3′-UTR in HEK293T cells transfected with miR-10a-5p mimic or miR-NC. (**C**) Quantification of mRNA expression of BDNF measured by qRT-PCR. GAPDH mRNA levels were used for normalization. (**D**) Histograms showed the ELISA analysis results of BDNF protein expression. (**E**) Relative mRNA expression of osteogenic markers ALP, RUNX2 and OCN in PDLCs cultured in GM, OM, OM with 50 ng/mL BDNF and OM with 100 ng/mL BDNF. GAPDH was used for normalization. (**F**) Western blot analysis of protein expression of RUNX2 and the internal control β-Actin in the above-mentioned groups. Histograms show the quantification of band intensities. β-Actin was used for normalization. (**G**) Images of ALP staining and ARS staining. Histograms show ALP activity and quantification of ARS staining by spectrophotometry. Scale bar, 100 μm. (**H**) Schematic of pathways involved in promoting PDLCs osteogenic differentiation by lncPVT1. lncPVT1 relieved the negative regulation of miR-10a-5p on BDNF and subsequently promoted osteogenesis (*$P < 0.05$; $^{\dagger}P < 0.01$). GM, growth medium; OM, osteogenic medium

involved in osteoblast differentiation of PDLCs. Moreover, overexpression of lncPVT1 promoted osteogenesis whereas knockdown decreased the osteogenic potential of PDLCs. LncRNAs are important molecules involved in the regulation of various cell activities,[12] however, only a few have been reported to participate in osteogenesis of dental tissue-derived stem cells.[16,25–27] LncPVT1 is a well-identified lncRNA.[28] Although its importance has been widely studied in many diseases, including cancer, cardiovascular disease and immune disease,[19,28,29] its role in osteogenesis has remained unclear. Here, we demonstrated its positive regulatory effect on the osteogenesis of PDLCs. Improving the osteogenic differentiation ability of PDLCs has been the focus of many studies,[30,31] our findings may provide a new molecular target for promoting osteogenesis.

We showed that lncPVT1 promotes the osteoblast differentiation of PDLCs by regulating miR-10a-5p.LncRNAs and miRNAs are known to affect each other and form a complex regulatory network that regulates gene expression.[32–35] LncPVT1 promotes the malignant behavior of ovarian cancer cells by acting as an miR-370 sponge;[36] its role as a molecular sponge of miR-26b is also important in the progression of hyperglycemia-induced collagen degradation.[37] In this study, we analyzed differentially expressed miRNAs in lncPVT1 knockdown and control cells via RNA-seq. Bioinformatics analysis suggested that lncPVT1 promoted the osteoblast differentiation of PDLCs by binding to miR-10a-5p, which is involved in cell proliferation,[38] apoptosis,[39] and the progression of osteoarthritis and cancers.[40,41] A previous study showed that miR-10a-5p could inhibit the osteogenic differentiation of bone mesenchymal stem cells (BMSCs).[42] Here, we revealed the binding potential of lncPVT1 and miR-10a-5p using the RIP assay. Besides, miR-10a-5p was significantly downregulated during osteogenesis and negatively correlated with the expression level of lncPVT1. Using overexpression and knockdown experiments, we determined that miR-10a-5p inhibited the osteoblastic differentiation of PDLCs. Further, miR-10a-5p partially reversed the stimulatory effects of lncPVT1 on osteogenesis, indicating involvement of the lncPVT1/miR-10a-5p regulatory network in the osteogenic differentiation of PDLCs.

We showed that lncPVT1/miR-10a-5p regulates the osteoblastic differentiation of PDLCs by targeting BDNF. BDNF, a member of the neurotrophin family, was originally identified as a growth factor for neuronal cells and was detected in both central and peripheral neuronal tissue.[43,44] Additionally, it is also synthesized and released by non-neuronal cells, such as fibroblasts, osteoblasts, and endothelial cells.[45] The effect of BDNF on angiogenesis and new bone formation in the process of fracture healing has been gradually clarified.[46] Here, the 3′-UTR region of BDNF was predicted to contain a putative miR-10a-5p binding site. We confirmed that the overexpression of miR-10a-5p significantly decreased luciferase reporter activity, whereas mutation of the binding site efficiently rescued the inhibitory effect of miR-10a-5p. Further, overexpression of lncPVT1 and knockdown of miR-10a-5p significantly increased BDNF expression, whereas knockdown of lncPVT1 and overexpression of miR-10a-5p decreased BDNF expression. Moreover, when lncPVT1 and miR-10a-5p were overexpressed simultaneously in PDLCs, the expression of BDNF did not change significantly. These results confirmed that BDNF was a downstream target of lncPVT1/miR-10a-5p.

Besides, we found that treatment with BDNF increased the osteogenic potential of PDLCs. A study based on BMSCs reached a similar conclusion.[47] However, the concentration that resulted in the strongest osteogenic ability in our study differed from that study; this may be related to differences in stem cell sources. Further, we confirmed BDNF treatment partially rescued the inhibitory effects of si-lncPVT1 on osteogenic differentiation, indicating that lncPVT1/miR-10a-5p regulated the osteoblastic differentiation of PDLCs by targeting BDNF. Previous studies have found that neuropeptides can regulate bone metabolism and promote osteogenesis by binding receptors on bone cells; the nervous system can also indirectly affect local bone metabolism by regulating blood flow.[48,49] Neurotrophins are also expressed in human periodontal tissue and may contribute to regeneration as well as innervation of periodontal tissue through local autocrine and paracrine pathways.[50] Thus, lncPVT1 could be related to the osteogenesis of PDLCs by affecting the expression of BDNF, and might be involved in the remodeling of periodontal tissue.

LncRNAs participate in gene expression regulation at multiple levels and via precise regulatory networks. Other mechanisms may be involved in the lncPVT1-mediated osteogenesis. In this study, we focused on its regulation of miR-10a-5p and BDNF, however, further studies are still needed. In addition, subsequent animal experiments are also necessary to verify the role of lncPVT1 in periodontal tissue regeneration in vivo.

5 | CONCLUSION

Our results suggest that lncPVT1promotes the osteoblast differentiation of PDLCs. Mechanistically, lncPVT1relieved the negative regulation of miR-10a-5p on BDNF and subsequently promoted osteogenesis (Figure 6H). This regulatory network may provide a novel approach to promote the osteogenic potential of PDLCs and aid in periodontal regeneration.

ACKNOWLEDGMENTS

This study was financially supported by grants from the National Natural Science Foundation of China, Beijing, China (No. 82071142, 82071119). Yunfei Zheng and Weiran Li are the co-corresponding authors.

CONFLICTS OF INTEREST

The authors have no conflicts of interest to disclose.

DATA AVAILABILITY STATEMENT

The data that support the findings of this study are available from the corresponding author upon reasonable request.

ORCID

Xiaobei Li https://orcid.org/0000-0003-2913-6895
Yiping Huang https://orcid.org/0000-0002-9230-1825
Yineng Han https://orcid.org/0000-0002-8651-3282
Qiaolin Yang https://orcid.org/0000-0003-2987-1881
Yunfei Zheng https://orcid.org/0000-0003-1899-8051
Weiran Li https://orcid.org/0000-0002-6635-6881

REFERENCES

1. Cochran DL. Inflammation and bone loss in periodontal disease. *J Periodontol*. 2008;79:1569-1576.
2. Di Benedetto A, Gigante I, Colucci S, Grano M. Periodontal disease: linking the primary inflammation to bone loss. *Clin Dev Immunol*. 2013;2013:503754.
3. Van Dyke TE. The management of inflammation in periodontal disease. *J Periodontol*. 2008;79:1601-1608.
4. Seo BM, Miura M, Gronthos S, et al. Investigation of multipotent postnatal stem cells from human periodontal ligament. *Lancet*. 2004;364:149-155.
5. Park JY, Jeon SH, Choung PH. Efficacy of periodontal stem cell transplantation in the treatment of advanced periodontitis. *Cell Transplant*. 2011;20:271-285.
6. Menicanin D, Mrozik KM, Wada N, et al. Periodontal-ligament-derived stem cells exhibit the capacity for long-term survival, self-renewal, and regeneration of multiple tissue types in vivo. *Stem Cells Dev*. 2014;23:1001-1011.
7. Liu Y, Zheng Y, Ding G, et al. Periodontal ligament stem cell-mediated treatment for periodontitis in miniature swine. *Stem Cells*. 2008;26:1065-1073.
8. Yu B, Hu J, Li Q, Wang F. CircMAP3K11 contributes to proliferation, apoptosis and migration of human periodontal ligament stem cells in inflammatory microenvironment by regulating TLR4 via miR-511 sponging. *Front Pharmacol*. 2021;12:633353.
9. Li X, Zhang B, Wang H, et al. The effect of aging on the biological and immunological characteristics of periodontal ligament stem cells. *Stem Cell Res Ther*. 2020;11:326.
10. Zhou Y, Fan W, Xiao Y. The effect of hypoxia on the stemness and differentiation capacity of PDLC and DPC. *Biomed Res Int*. 2014;2014:890675.
11. Cech TR, Steitz JA. The noncoding RNA revolution-trashing old rules to forge new ones. *Cell*. 2014;157:77-94.
12. Batista PJ, Chang HY. Long noncoding RNAs: cellular address codes in development and disease. *Cell*. 2013;152:1298-1307.
13. Chen J, Wang Y, Wang C, Hu JF, Li W. LncRNA functions as a new emerging epigenetic factor in determining the fate of stem cells. *Front Genet*. 2020;11:277.
14. Zheng Y, Li X, Huang Y, Jia L, Li W. Time series clustering of mRNA and lncRNA expression during osteogenic differentiation of periodontal ligament stem cells. *Peer J*. 2018;6:e5214.
15. Liu Z, Xu S, Dao J, Gan Z, Zeng X. Differential expression of lncRNA/miRNA/mRNA and their related functional networks during the osteogenic/odontogenic differentiation of dental pulp stem cells. *J Cell Physiol*. 2020;235:3350-3361.
16. Huang Y, Han Y, Guo R, et al. Long non-coding RNA FER1L4 promotes osteogenic differentiation of human periodontal ligament stromal cells via miR-874-3p and vascular endothelial growth factor A. *Stem Cell Res Ther*. 2020;11:5.
17. Jia B, Qiu X, Chen J, et al. A feed-forward regulatory network lncPCAT1/miR-106a-5p/E2F5 regulates the osteogenic differentiation of periodontal ligament stem cells. *J Cell Physiol*. 2019;234:19523-19538.
18. Chen Q, Cao M, Ge H. Knockdown of MALAT1 inhibits the progression of chronic periodontitis via targeting miR-769-5p/HIF3A axis. *Biomed Res Int*. 2021;2021:8899863.
19. Cho SW, Xu J, Sun R, et al. Promoter of lncRNA gene PVT1 is a tumor-suppressor DNA boundary element. *Cell*. 2018;173:1398-1412 e1322.
20. Sun B, Meng M, Wei J, Wang S. Long noncoding RNA PVT1 contributes to vascular endothelial cell proliferation via inhibition of miR-190a-5p in diagnostic biomarker evaluation of chronic heart failure. *Exp Ther Med*. 2020;19:3348-3354.
21. Zhang CW, Wu X, Liu D, et al. Long non-coding RNA PVT1 knockdown suppresses fibroblast-like synoviocyte inflammation and induces apoptosis in rheumatoid arthritis through demethylation of sirt6. *J Biol Eng*. 2019;13:60.
22. Zheng Y, Li X, Huang Y, Jia L, Li W. The circular RNA landscape of periodontal ligament stem cells during osteogenesis. *J Periodontol*. 2017;88:906-914.
23. Leng N, Dawson JA, Thomson JA, et al. EBSeq: an empirical Bayes hierarchical model for inference in RNA-seq experiments. *Bioinformatics*. 2013;29:1035-1043.
24. Li X, Zheng Y, Zheng Y, et al. Circular RNA CDR1as regulates osteoblastic differentiation of periodontal ligament stem cells via the miR-7/GDF5/SMAD and p38 MAPK signaling pathway. *Stem Cell Res Ther*. 2018;9:232.
25. Zhou M, Hu H, Han Y, et al. Long non-coding RNA 01126 promotes periodontitis pathogenesis of human periodontal ligament cells via miR-518a-5p/HIF-1alpha/MAPK pathway. *Cell Prolif*. 2021;54:e12957.
26. Yang Q, Han Y, Liu P, et al. Long noncoding RNA GAS5 promotes osteogenic differentiation of human periodontal ligament stem cells by regulating GDF5 and p38/JNK signaling pathway. *Front Pharmacol*. 2020;11:701.
27. Qiu W, Wu BL, Fang FC. Overview of noncoding RNAs involved in the osteogenic differentiation of periodontal ligament stem cells. *World J Stem Cells*. 2020;12:251-265.
28. Tseng YY, Moriarity BS, Gong W, et al. PVT1 dependence in cancer with MYC copy-number increase. *Nature*. 2014;512:82-86.

29. Hu F, Tao X, Zhao L, et al. LncRNA-PVT1 aggravates severe acute pancreatitis by promoting autophagy via the miR-30a-5p/Beclin-1 axis. *Am J Transl Res*. 2020;12:5551-5562.
30. Zhang LN, Wang XX, Wang Z, Li KY, Xu BH, Zhang J. Berberine improves advanced glycation end productsinduced osteogenic differentiation responses in human periodontal ligament stem cells through the canonical Wnt/betacatenin pathway. *Mol Med Rep*. 2019;19:5440-5452.
31. Zhang W, Jia L, Zhao B, et al. Quercetin reverses TNFalpha induced osteogenic damage to human periodontal ligament stem cells by suppressing the NFkappaB/NLRP3 inflammasome pathway. *Int J Mol Med*. 2021;47:39.
32. Anastasiadou E, Jacob LS, Slack FJ. Non-coding RNA networks in cancer. *Nat Rev Cancer*. 2018;18:5-18.
33. Panni S, Lovering RC, Porras P, Orchard S. Non-coding RNA regulatory networks. *Biochim Biophys Acta Gene Regul Mech*. 2020;1863:194417.
34. Tay Y, Rinn J, Pandolfi PP. The multilayered complexity of ceRNA crosstalk and competition. *Nature*. 2014;505:344-352.
35. Kazimierczyk M, Kasprowicz MK, Kasprzyk ME, Wrzesinski J. Human long noncoding RNA interactome: detection, characterization and function. *Int J Mol Sci*. 2020;21:1027.
36. Yi K, Hou M, Yuan J, et al. LncRNA PVT1 epigenetically stabilizes and post-transcriptionally regulates FOXM1 by acting as a microRNA sponge and thus promotes malignant behaviors of ovarian cancer cells. *Am J Transl Res*. 2020;12:2860-2874.
37. Ding LB, Li Y, Liu GY, et al. Long non-coding RNA PVT1, a molecular sponge of miR-26b, is involved in the progression of hyperglycemia-induced collagen degradation in human chondrocytes by targeting CTGF/TGF-beta signal ways. *Innate Immun*. 2020;26:204-214.
38. Vaher H, Runnel T, Urgard E, et al. miR-10a-5p is increased in atopic dermatitis and has capacity to inhibit keratinocyte proliferation. *Allergy*. 2019;74:2146-2156.
39. Ma Y, Wu Y, Chen J, et al. miR-10a-5p promotes chondrocyte apoptosis in osteoarthritis by targeting HOXA1. *Mol Ther Nucleic Acids*. 2019;14:398-409.
40. Li HZ, Xu XH, Lin N, et al. Overexpression of miR-10a-5p facilitates the progression of osteoarthritis. *Aging (Albany NY)*. 2020;12:5948-5976.
41. Worst TS, Previti C, Nitschke K, et al. miR-10a-5p and miR-29b-3p as extracellular vesicle-associated prostate cancer detection markers. *Cancers (Basel)*. 2019;12:43.
42. Zhang Y, Zhou L, Zhang Z, Ren F, Chen L, Lan Z. miR10a5p inhibits osteogenic differentiation of bone marrowderived mesenchymal stem cells. *Mol Med Rep*. 2020;22:135-144.
43. Hohn A, Leibrock J, Bailey K, Barde YA. Identification and characterization of a novel member of the nerve growth factor/brain-derived neurotrophic factor family. *Nature*. 1990;344:339-341.
44. Kim H, Li Q, Hempstead BL, Madri JA. Paracrine and autocrine functions of brain-derived neurotrophic factor (BDNF) and nerve growth factor (NGF) in brain-derived endothelial cells. *J Biol Chem*. 2004;279:33538-33546.
45. Sariola H. The neurotrophic factors in non-neuronal tissues. *Cell Mol Life Sci*. 2001;58:1061-1066.
46. Kilian O, Hartmann S, Dongowski N, et al. BDNF and its TrkB receptor in human fracture healing. *Ann Anat*. 2014;196:286-295.
47. Liu Q, Lei L, Yu T, Jiang T, Kang Y. Effect of brain-derived neurotrophic factor on the neurogenesis and osteogenesis in bone engineering. *Tissue Eng Part A*. 2018;24:1283-1292.
48. Masi L. Crosstalk between the brain and bone. *Clin Cases Miner Bone Metab*. 2012;9:13-16.
49. Qiao Y, Wang Y, Zhou Y, et al. The role of nervous system in adaptive response of bone to mechanical loading. *J Cell Physiol*. 2019;234:7771-7780.
50. Kurihara H, Shinohara H, Yoshino H, Takeda K, Shiba H. Neurotrophins in cultured cells from periodontal tissues. *J Periodontol*. 2003;74:76-84.

SUPPORTING INFORMATION

Additional supporting information may be found in the online version of the article at the publisher's website.

How to cite this article: Li X, Huang Y, Han Y, Yang Q, Zheng Y, Li W. LncPVT1 regulates osteogenic differentiation of human periodontal ligament cells via miR-10a-5p/brain-derived neurotrophic factor. *J Periodontol*. 2022;1-14. https://doi.org/10.1002/JPER.21-0429